

THEORETICAL AND EXPERIMENTAL ANALYSIS OF MIXED EXCITON-POLARITON LUMINESCENCE IN *CdS* CRYSTALS IN THE REGIME OF STRONG EXCITON DAMPING

✉ **Bozorboy J. Akhmadaliev**, ✉ **Mekhriddin F. Akhmadjonov**, ✉ **Tokhirbek I. Rakhmonov***,
 ✉ **Paxlovon I. Movlonov**, ✉ **Sherzod Sh. Abdullaev**, ✉ **Iftikhorjon I. Yulchiev**

Fergana State Technical University, Fergana, Uzbekistan

*Corresponding Author e-mail: radiofizik2014@gmail.com

Received March 2, 2026; revised April 23, 2026; accepted April 28, 2026

This work presents a combined theoretical and experimental study of mixed exciton-polariton luminescence in anisotropic *CdS* crystals in the regime of strong exciton damping near the A-exciton resonance. A spatially dispersive model of radiative mixed modes is used to analyze the transformation of the spectral contour, peak position, partial modal contributions, and angular dependence of the linewidth. Calculated spectra for emission angles from 10.4° to 85° are compared with photoluminescence measurements, and good agreement is obtained at $T \approx 77$ K for $\hbar\Gamma = 2.0$ meV and $L = 0.85$ μm . Unlike conventional approaches that relate the transition to a Lorentzian emission profile only to the condition $\Gamma \gg \Gamma_c$, we show that this regime additionally requires the transport-related constraint $2k_0L \cdot \text{Im} n_{Mz} \ll 1$. Under these combined conditions, the mixed-mode emission contour approaches a quasiclassical Lorentzian profile with a half-width close to $\hbar\Gamma$. At the same time, spatial dispersion and intermode interference are not fully suppressed in anisotropic *CdS* crystals and become more pronounced at larger emission angles or smaller effective diffusion lengths. The results provide a refined criterion for identifying the quasiclassical emission regime and a practical framework for extracting exciton damping and effective diffusion depth from experimental spectra.

Keywords: *Mixed exciton-polariton luminescence; CdS crystal; Strong exciton damping; Spatial dispersion; Anisotropic semiconductor; Mixed modes; A-exciton resonance*

PACS: 71.36.+c, 71.35.Cc, 78.55.Et, 78.20.Bh, 78.20.Ci

INTRODUCTION

Exciton-polaritons arise from the strong coupling between resonant optical fields and excitonic excitations in crystals, and their spectral response near exciton resonances cannot be adequately described within a purely local dielectric framework [1-3]. In anisotropic semiconductors such as *CdS*, this light-matter interaction is further complicated by polarization-dependent mode mixing, boundary-transmission effects, and spatial dispersion, which together give rise to nonclassical optical phenomena in absorption, transmission, and emission spectra [2-6].

CdS has long been regarded as a model material for bulk exciton-polariton optics because of its pronounced optical anisotropy, relatively strong excitonic oscillator strength, and well-resolved A-exciton resonance at low temperatures [5-9]. Early transmission and luminescence studies showed that, in *CdS* single crystals, the spectral shape and angular behavior of excitonic emission are governed not by a simple local-exciton emission mechanism, but by the structure of the polariton branches [7-8]. Subsequent studies of damping dispersion demonstrated that the excitonic dephasing rate in *CdS* depends on both frequency and temperature, reflecting the influence of distinct impurity- and phonon-assisted relaxation channels [8-11]. These results make *CdS* particularly suitable for analyzing how dissipative decay modifies the observable manifestations of exciton-polariton coupling.

At the same time, the regime of strong exciton damping remains a theoretically and experimentally nontrivial problem. When the dissipative decay of excitons becomes comparable to or exceeds the characteristic polaritonic energy scales, the emission spectrum may approach a quasiclassical Lorentzian contour. However, in uniaxial crystals this transition is not complete, since spatial-dispersion effects, additional radiative waves, and interference between mixed modes may still remain observable, particularly at oblique emission angles. Recent studies on *CdS*-type crystals have shown that surface-radiative and longitudinal-exciton contributions are often smaller than the dominant bulk mixed-mode contribution; nevertheless, they are indispensable for achieving quantitative agreement with experiment and for explaining the appearance of additional spectral features near the longitudinal resonance frequency [12-13].

Despite these advances, the conditions under which mixed exciton-polariton luminescence acquires a quasiclassical Lorentzian profile remain insufficiently clarified. In most previous works, this transition is primarily associated with the condition $\Gamma \gg \Gamma_c$. However, such an interpretation does not fully account for the role of spatial dispersion, finite exciton transport, and boundary-induced mode conversion, which can significantly influence the spectral formation.

In this work, we demonstrate that the realization of the Lorentzian regime requires not only strong exciton damping but also an additional condition related to the effective diffusion length of polaritons. We show that the interplay between damping, spatial dispersion, and finite transport leads to a nontrivial angular evolution of the emission spectrum, which cannot be explained within conventional local approaches.

Therefore, a consistent description of mixed exciton-polariton luminescence in the strong-damping regime is important for both fundamental solid-state optics and the interpretation of experimental spectra. Such a description makes it possible to distinguish the roles of damping, interference, and spatial dispersion, and to extract physically meaningful parameters such as the exciton decay constant, effective diffusion depth, angular evolution of the linewidth, and the relative weights of partial radiative contributions [10-13]. This problem is especially relevant in anisotropic crystals, where the crystal boundary and mode conversion strongly influence which mixed states can radiate into the external medium [3-5].

In this work, we present a theoretical and experimental analysis of mixed exciton-polariton luminescence in *CdS* crystals in the regime of strong exciton damping. The study is focused on the transformation of the spectral contour, linewidth, peak position, and partial modal contributions of the emitted radiation near the A-exciton resonance under different emission angles and damping conditions. By comparing calculated integral and partial spectra with experimental luminescence data, this work clarifies the conditions under which the spectrum approaches a classical Lorentzian form and those under which spatial-dispersion and interference effects continue to govern the observed emission, thereby providing a more rigorous physical basis for describing mixed-mode radiation in strongly dissipative excitonic systems.

METHODOLOGY

Mixed exciton-polariton luminescence in *CdS* crystals was analyzed within a combined theoretical, numerical, and experimental framework appropriate for the regime of strong exciton damping. The spectral behavior in the vicinity of the $A_{n=1}$ exciton resonance was described using the dispersion model of radiative mixed modes in a spatially dispersive crystal. Within this approach, the luminescence contour is determined by the coupled excitonic and electromagnetic response of the medium, while exciton damping, anomalous dispersion, modal interference, and boundary-related radiative effects are treated explicitly in the spectral formalism.

The theoretical analysis was performed for the limiting case of very strong exciton damping, where the contribution of spatial dispersion and light-exciton interaction is substantially weakened relative to dissipative broadening. Under these conditions, the total luminescence intensity was represented in a reduced form that makes it possible to separate the dominant radiative contribution from secondary terms and to trace the evolution of the emission contour toward a quasi-classical Lorentzian profile. Accordingly, the spectral half-width of the mixed-mode luminescence line was analyzed as a function of the damping parameter and the transport characteristics of the radiative states.

The numerical part of the study was based on calculations of both the integral luminescence spectra and their partial components in the spectral region of the $A_{n=1}$ exciton resonance. The spectra were calculated for radiation exit angles $\theta = 10.4^\circ, 45^\circ, 60^\circ,$ and 85° . For the case $T \approx 77$ K, the calculations were performed with $\hbar\Gamma = 2.0$ meV using a common set of optical parameters. This procedure made it possible to evaluate the angular evolution of the spectral contour, including the position of the maximum, the degree of asymmetry, the role of interference terms, and the variation of the half-width with increasing observation angle.

Experimental verification was carried out by comparing the calculated spectra with photoluminescence data obtained for *CdS* crystals near the $A_{n=1}$ exciton resonance. The spectrum measured at $T = 77$ K and $\theta = 10.4^\circ$ was fitted by the theoretical contour calculated from the model equations. In the fitting procedure, the damping parameter Γ was taken equal to the experimentally observed half-width of the A-line at the corresponding temperature, whereas the effective diffusion length L of the upper-branch polaritons was determined from the angular dependence of the A_L emission line by comparison with the calculated spectra. For the spectrum recorded at $T = 77$ K, the fitting was performed using $\hbar\Gamma = 2.0$ meV, $\ell = 70$ Å and $L = 0.85$ μm.

Since the emission spectrum in the exciton-resonance region contains a background contribution that is not directly related to the A_L -line formation mechanism, the background component was introduced separately in the comparison between theory and experiment. Therefore, the final theoretical contour was considered with the corresponding background-intensity correction. The remaining deviation between theory and experiment in the short-wavelength part of the spectrum was attributed to inelastic scattering processes of polaritons that were not included in the basic approximation.

The validity of the model was further tested by analyzing the angular dependence of the spectral half-width $\Delta(\theta)$ of the mixed-mode emission line at $T = 4.5, 15, 44,$ and 77 K. The comparison between theoretical and experimental $\Delta(\theta)$ dependences was carried out using the parameter sets $L = 1.5, 1.7, 1.6, 0.85$ μm and $\Gamma = 0.1, 0.2, 0.5, 2.0$ meV, respectively. This procedure made it possible to determine the temperature and angular intervals in which mixed-mode luminescence approaches classical Lorentzian behavior and to evaluate the applicability of the line half-width as a practical indicator of exciton damping and crystal quality.

RESULTS AND DISCUSSION

Based on our theoretical calculations, we now analyze the partial contributions to the total luminescence intensity given by

$$I_p^{(0)}(\omega, \vec{\Omega}) = C \cdot \frac{4n_{ox}^2 n_{oz} L_{cr}}{|N_M|^2} \cdot \Gamma_f(\omega) \quad (1)$$

and examine several characteristic features of the spectrum $I_p^{(0)}(\omega, \theta)$ in the corresponding limiting case. Under these conditions, the effects of spatial dispersion (SD) and light-exciton interaction become substantially weaker than the exciton damping processes, and damping acquires the dominant role in the formation of mixed exciton-polariton luminescence (MEPL).

Thus, neglecting the contribution of the second branch, the spectral intensity of mixed exciton-polariton luminescence (MEPL) can be written in the form

$$I_p^{(0)}(\omega, \vec{\Omega}) \cong C \cdot \frac{4n_{ox}^2 n_{oz}}{|n_{M1}^2 - n_{M2}^2|^2} \left| \frac{n_{M1z} + n_{M2z}}{1 + \tilde{n}_p} \right|^2 \cdot \frac{\Gamma_f(\omega)}{2k_0 \operatorname{Im} n_{Mz} + L^{-1}}, \quad (2)$$

where n_{Mz} is the refractive index having the smallest absolute value among n_{M1z} and n_{M2z} .

$$n_{M\beta}^2(\omega, \theta) = \frac{1}{2} \left\{ \left(1 - \frac{M_{\perp}}{M_{\parallel}} \right) \sin^2 \theta + \frac{\omega - \omega_L + i\Gamma/2}{\omega_{M\perp}} + \varepsilon_b - (-1)^\beta \left[\left(\left(1 - \frac{M_{\perp}}{M_{\parallel}} \right) \sin^2 \theta + \frac{\omega - \omega_L + i\Gamma/2}{\omega_{M\perp}} - \varepsilon_b \right)^2 + 4 \frac{\omega_{LT}}{\omega_{M\perp}} \sin^2 \theta \right]^{1/2} \right\}, \beta = 1, 2. \quad (3)$$

Proceeding from this dispersion equation, it can be shown that in the case $\Gamma \gg \Gamma_c$, the following relation holds:

$$|n_{M1}^2 - n_{M2}^2|^2 = \frac{(\omega - \omega_c)^2 + \Gamma^2/4}{\omega_{M\perp}^2}. \quad (4)$$

Taking Eq. (4) into account, expression (2) can be reduced to the final form

$$I_p^{(0)}(\omega, \vec{\Omega}) \cong \frac{k_0^2}{(2\pi)^3} \hbar\omega \cdot \frac{2n_{0x}^2 n_{0z} \varepsilon_b \omega_{LT}}{(\omega - \omega_c)^2 + \Gamma^2/4} \left| \frac{n_{M1z} + n_{M2z}}{1 + \tilde{n}_p} \right|^2 \cdot \frac{k_0 L \Gamma_f(\omega)}{2k_0 L \operatorname{Im} n_{Mz} + 1}. \quad (5)$$

The calculations show that when $\Gamma \gg \Gamma_c$, the factor $\left| \frac{n_{M1z} + n_{M2z}}{1 + \tilde{n}_p} \right|^2$ is almost independent of frequency (with an accuracy better than 0.5%). Therefore, when the following condition is satisfied,

$$2k_0 L \cdot \operatorname{Im} n_{Mz} \ll 1, \quad (6)$$

Eq. (5) describes “classical” radiation, for which the effects of spatial dispersion (SD) and light-exciton interaction are very small. For this reason, the appearance of a Lorentz-type denominator in Eq. (5) is quite natural. When $\Gamma \gg \Gamma_c$ and condition (6) is fulfilled, this denominator predominantly determines the shape of the radiation spectrum. In this case, the spectral half-width Δ_A of the luminescence line of the mixed modes corresponds to $\hbar\Gamma$.

It should be emphasized here that, for the radiation of mixed modes to become fully “classical,” the condition $\Gamma \gg \Gamma_c$ alone is not sufficient. As follows from Eq. (5), the inequality (6) must also be strictly satisfied. In the frequency range $\omega \geq \omega_c$, when $n_{Mz} = n_{M2z}$, the following relation holds: $\operatorname{Im} n_{Mz} \cong \frac{\Gamma_c^2 / (\omega_{M1} \Gamma)}{16\sqrt{\varepsilon_b - \sin^2 \theta}} \cdot \frac{\Gamma^2/4}{(\omega - \omega_c)^2 + \Gamma^2/4}$.

Thus, when $\omega = \omega_c$, condition (6) takes the form of the following inequality:

$$\Gamma \gg \Gamma_c \frac{\Gamma_c k_0 L}{8\omega_{M1} \sqrt{\varepsilon_b - \sin^2 \theta}}, \quad \text{i.e.,} \quad L \gg \frac{8\omega_{M1} \sqrt{\varepsilon_b - \sin^2 \theta}}{\Gamma_c k_0}. \quad (7)$$

For the CdS crystal parameters, we take the following values into account:

$$\hbar\omega_{M1} = 0.007 \text{ meV}, \quad k_0 = 1.29 \cdot 10^5 \text{ cm}^{-1}, \quad \varepsilon_{b\perp} = 9.4.$$

From this, it follows that $\hbar\Gamma_{c\max} = 4\hbar\sqrt{\omega_{LT}\omega_{M1}} \approx 0.4753 \text{ meV}$.

Accordingly, one obtains $\frac{8\omega_{M1}\sqrt{\varepsilon_b-1}}{\Gamma_c k_0} \approx 0.02 \mu\text{m}$.

Hence, for such crystals under the condition $\Gamma \gg \Gamma_c$, inequality (7) is well satisfied when the exciton diffusion length is $L \approx 1.0 \mu\text{m}$.

However, when $L < 0.2 \mu\text{m}$, this inequality is violated and the condition $\Gamma \gg \Gamma_c$ is no longer fulfilled. In this case, spatial dispersion (SD) affects the shape of the luminescence contour.

If the initial quantum states $T1$ and $M1$ are sufficiently well defined, then

$$I_p^{(0)}(\omega, \vec{\Omega}) = \sum_{\beta=M1, M2} I_{p,\beta}^{(0)}(\omega, \vec{\Omega}) + I_{p,M12}^{(0)}(\omega, \vec{\Omega}) \quad (8)$$

$$I_{p,\beta}^{(0)}(\omega, \vec{\Omega}) = F(\omega, \vec{\Omega}) |F_\beta(\omega, \vec{\Omega})|^2 / (2k_0 \operatorname{Im} n_{\beta z} + L^{-1}) \quad (9)$$

$$I_{p,M12}^{(0)}(\omega, \vec{\Omega}) = -F(\omega, \vec{\Omega}) \cdot 2 \operatorname{Re} \left[\frac{F_{M1}(\omega, \vec{\Omega}) F_{M2}^*(\omega, \vec{\Omega})}{-ik_0(n_{M1z} - n_{M2z}) + L^{-1}} \right] \quad (10)$$

$$F(\omega, \vec{\Omega}) = \frac{1}{(2\pi)^3} \frac{2M_{\parallel}^2 c \varepsilon_b \omega_{LT} \cos \theta}{\hbar |n_{M1}^2 - n_{M2}^2|^2} \sum_{\beta'=T1, M1} \sum_{\vec{k}_{\beta'}} \frac{f_{\beta' \vec{k}_{\beta'}}(\omega)}{\tau_{M,\beta' \vec{k}_{\beta'}}(\omega)} \quad (11)$$

$$F_\beta(\omega, \vec{\Omega}) = \frac{t_{0\beta}^{(p)}(\omega, \vec{\Omega})}{n_{\beta z}} \left[\frac{(n_{\beta}^2 - \varepsilon_b)^2}{\varepsilon_b^2} \cdot \frac{n_{\beta z}^2}{n_{\beta}^2} + \frac{n_{0x}^2}{n_{\beta}^2} \right]^{1/2} \quad (12)$$

The above general theoretical relations obtained in our calculations, namely the equations describing mixed exciton-polariton luminescence (MEPL), remain valid in the case $\Gamma \gg \Gamma_c$ as well, since it is precisely under these conditions that scattering into the radiative $M1$ and $M2$ modes occurs.

Additional numerical calculations of the dispersion values of truncated normal waves for different values of Γ show that when $\Gamma \approx 2.0 \div 2.5 \text{ meV}$ ($T \approx 70 \div 80 \text{ K}$), the kinetic approach remains applicable in the vicinity of the frequency ω_L and above it, provided that the quasiclassical Boltzmann approach is not treated as an excessively restrictive requirement. In this case, the upper dispersion branch $T1$ can also be described within the quasiclassical approximation, and under these conditions strong damping of the mixed $M1$ and $M2$ modes is ensured through elastic and inelastic scattering of $T1$ polaritons.

Indeed, as shown in Fig. 1, at $T = 77 \text{ K}$ and $\theta = 10.4^\circ$, the experimental luminescence spectrum agrees well with the theoretical branch $I_p^{(0)}(\omega)$ calculated from Eqs. (8)-(12), where the values $\hbar\Gamma = 2.0 \text{ meV}$, $\ell = 70 \text{ \AA}$, and $L = 0.85 \mu\text{m}$ were used. (The results presented here and below were obtained within the framework of experimental studies carried out by Prof. A.V. Sel'kin.)

In this case, the effective diffusion length L of the upper-branch polaritons at $T = 77 \text{ K}$ was determined for the A_L line by comparing with the theoretical calculation results based on the angular dependence $\Delta(\theta)$.

Likewise, the value of Γ was taken to be equal to the half-width Δ_A of the emission line at this temperature. The dotted straight line describes the contribution of the crystal background emission in the spectral region of the $A_{n=1}$ exciton resonance and is not related to the emission mechanisms of the A_L line. The theoretical solid curve is presented with a correction introduced to the background

emission intensity. At the same time, in the short-wavelength part of the spectrum, a discrepancy of about 3-5% is observed between the theoretical and experimental results. This is associated with the fact that inelastic scattering in the $T1$ and $M1$ branches was not taken into account.

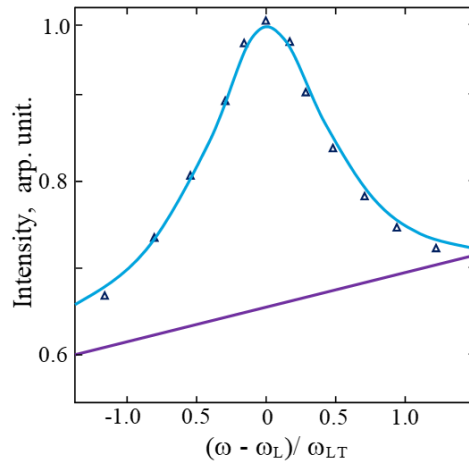


Figure 1. Experimental and theoretical comparison of the emission spectrum of mixed modes in a CdS crystal. The experimental data ($T = 77$ K, triangular symbols) and the theoretical curve (solid line), calculated for $\hbar\Gamma = 2.0$ meV, $\theta = 10.4^\circ$, and $L = 0.85 \mu\text{m}$, are shown. The dotted line represents the contribution of the crystal background emission in the spectral region of the $A_{n=1}$ exciton resonance.

In cases a, b, c , and d of Fig. 2, the theoretical spectra of the total (integral) and partial contributions to mixed exciton-polariton luminescence (MEPL) in a CdS crystal are presented. The solid line denotes the total (integral) spectrum, the dotted line represents the I_{M1} contribution, the dashed line corresponds to the I_{M2} contribution, and the dash-dotted line shows the I_{M12} contribution. The calculations were performed for the emission angles $\theta = 10.4^\circ$ (a), 45° (b), 60° (c), and 85° (d) at $\hbar\Gamma = 2.0$ meV ($T \approx 77$ K), using the same optical parameters as those employed for the theoretical spectrum in Fig. 1.

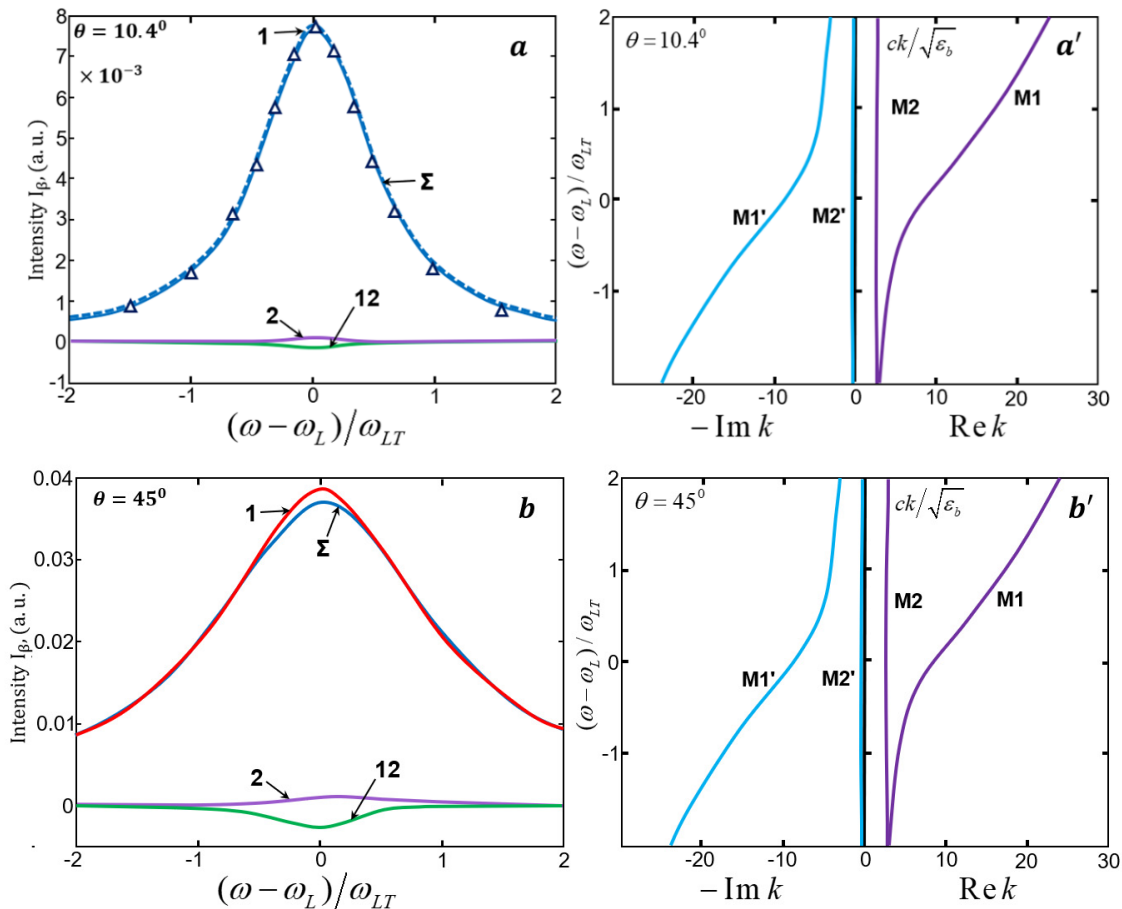


Figure 2. Theoretical photoluminescence spectra of mixed exciton-polariton modes in a CdS crystal ($a-d$) together with the corresponding dispersion curves ($a'-d'$), calculated for $\hbar\Gamma = 2.0$ meV ($T \approx 77$ K). The results are shown for emission angles into vacuum of $\theta = 10.4^\circ$ (a, a'), 45° (b, b'), 60° (c, c'), and 85° (d, d')
(continued on the next page)

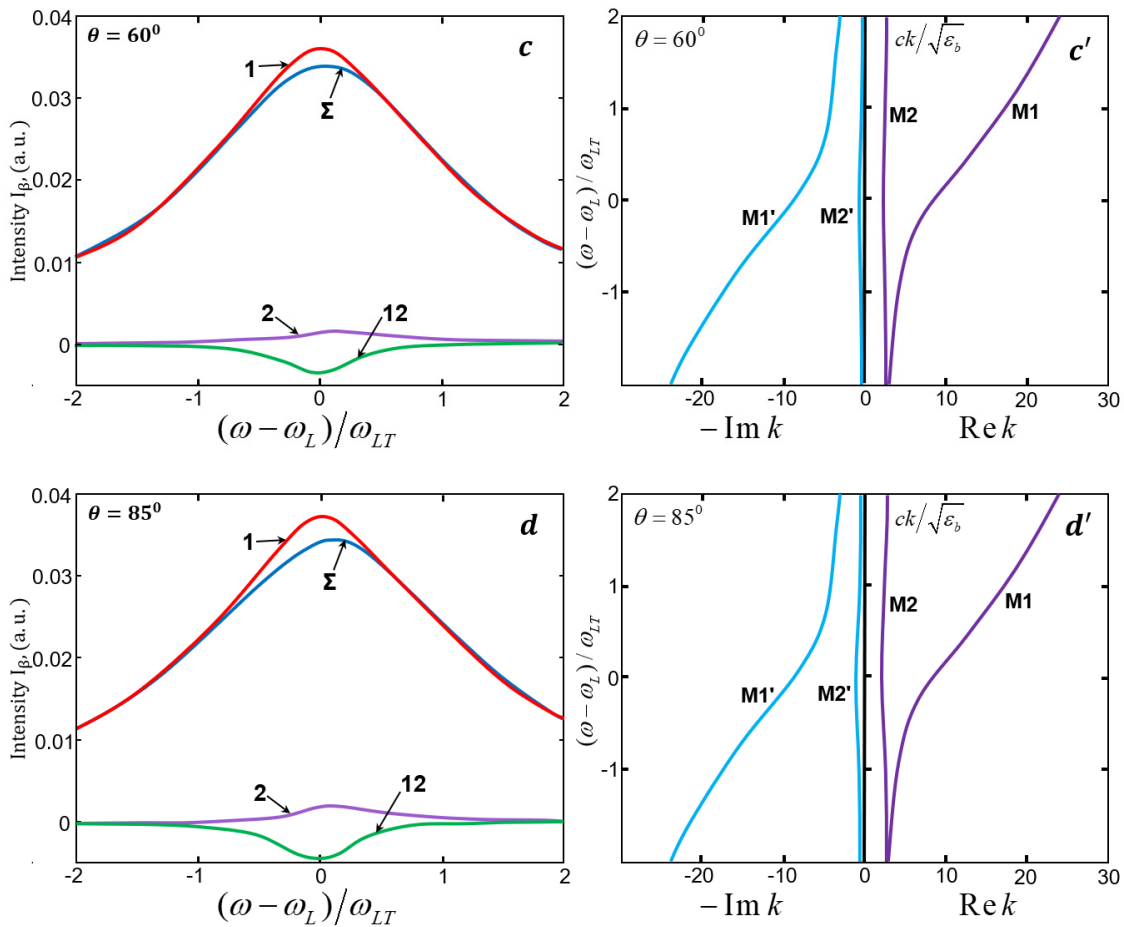


Figure 2. Theoretical photoluminescence spectra of mixed exciton-polariton modes in a CdS crystal (a-d) together with the corresponding dispersion curves (a'-d'), calculated for $\hbar\Gamma = 2.0$ meV ($T \approx 77$ K). The results are shown for emission angles into vacuum of $\theta = 10.4^\circ$ (a, a'), 45° (b, b'), 60° (c, c'), and 85° (d, d')

It is evident that, for the angle $\theta = 10.4^\circ$, the total spectrum $I_p^{(0)}(\omega, \theta)$ and the partial spectrum $I_{M1}^{(0)}(\omega, \theta)$ coincide to within 98% accuracy and form a symmetric Lorentz contour with a maximum at the longitudinal frequency ω_L . The half-width of the line is $\Delta(10.4^\circ) \approx 2.0$ meV. This agrees very well with the corresponding regime of MEPL formation under the condition $\Gamma \gg \Gamma_c$, with $\gamma_{SD} \approx 0.04$ and $\gamma_{LT} \approx 0.01$ [13].

In this case, the maximum combined contribution of $I_{M2}^{(0)}$ and $I_{M12}^{(0)}$ does not exceed 2%. However, at the angles 45° , 60° , and 85° , this contribution amounts to 7%, 10%, and 15%, respectively, which reflects the significant role of spatial dispersion (SD) ($\gamma_{SD} \approx 0.17, 0.20, 0.23$, and $\gamma_{LT} \approx 0.06, 0.08, 0.10$).

It should be emphasized that in this case ($\hbar\Gamma = 2$ meV and $\theta \geq 45^\circ$), MEPL is actually formed when the following conditions are satisfied: $\Gamma \geq \Gamma_c$, $\Gamma \gg \tilde{\omega}_{LT}$. Under these conditions, only the polariton effect is partially screened by damping, whereas anomalous dispersion and the interference contribution $I_{M\beta}^{(0)}$ continue to influence the shape of the spectral contour $I_p^{(0)}$. Thus, with increasing θ , the maximum of the A_L line shifts from ω_L toward the short-wavelength side (due to the inclusion of the $I_{M2}^{(0)}$ contribution). At the same time, the asymmetry and the half-width of the A_L line increase systematically (compare cases a – d and a' – d' in Fig. 2). Meanwhile, the minimum value of the spectral line $I_{M12}^{(0)}$ (at ω_L) and its half-width (≈ 2.0 meV) are almost independent of θ .

As the crystal temperature increases, the corresponding increase in Γ makes it possible to observe a transformation of the MEPL spectrum caused by dissipative exciton damping. In particular, characteristic features are manifested in the dependence of the half-width Δ_A of the mixed-mode emission line in a CdS crystal on temperature and on the emission angle θ .

As can be seen from Fig. 3, the theoretical and experimental $\Delta(\theta)$ curves corresponding to different temperatures ($T = 4.5$ (1), 15 (2), 44 (3), 77 (4) K) differ significantly from one another. First of all, attention is drawn to the horizontal segments of these curves, whose length increases with increasing temperature. Comparing the measured values of Γ for CdS samples [14] with the values of $\Gamma_c(\theta)$, one finds that the above-mentioned horizontal segments of the $\Delta(\theta)$ curves correspond to the condition $\Gamma \gg \Gamma_c$, i.e., strong damping of mechanical excitons is observed.

For the “classical” radiation shown in panel (a) of Fig. 2 (a, b, c, d), i.e., radiation described by Lorentz oscillators, the corresponding θ values are in close agreement with the horizontal segments of the $\Delta(\theta)$ curves in Fig. 3, provided that $\Gamma \gg \Gamma_c$ and $\Delta \approx \Gamma$, that is, when the half-width does not depend on θ . This conclusion is of practical importance.

In the above Fig. 2, comparison plots of the dispersion curves of mixed modes (a' – d') and the photoluminescence spectra (a – d) are presented for $\Gamma = 2.0$ meV. For a CdS crystal at $\hbar\Gamma = 2.0$ meV ($T \approx 77$ K), with emission angles into vacuum $\theta = 10.4^\circ$ (a), 45° (b), 60° (c), and 85° (d), the total (solid) and partial contributions to mixed exciton-polariton luminescence are shown in

panels (a – d): I_{M1} (red), I_{M2} (purple), and I_{M12} (green). The triangles represent the experimental points from Fig. 1 (with the background-emission contribution excluded, $T = 77$ K).

The measurement of the half-width of the A_L line in the emission of mixed exciton-polariton modes (MEPM) at small emission angles θ is the simplest method for determining the values of the parameter $\hbar\Gamma$ near the frequency ω_L over a wide temperature range. It should be taken into account, however, that any structural imperfections of the crystal also contribute to the value of Γ . Therefore, the half-width of the mixed-mode emission line can serve as a simple and reliable criterion for evaluating sample quality in the classical case. A detailed analysis carried out previously shows that, compared with methods for determining Γ from transmission and reflection spectra, the determination of Γ from the half-width of the A_L line in MEPL is a more reliable approach when the temperature of CdS samples exceeds 60 K.

Thus, the theoretical and experimental analysis performed in this work demonstrates that, in anisotropic CdS crystals, strong dissipative damping of mixed exciton-polariton modes leads to a substantial transformation of the MEPL spectra. In the regime $\Gamma \gg \Gamma_c$, the spectral contour approaches a quasiclassical Lorentzian form only if the additional condition expressed by Eq. (6) [Eq. (7)] is also satisfied. In this limit, dissipative broadening becomes dominant, whereas the influence of spatial dispersion and light-exciton interaction on the spectral contour is substantially reduced. However, when the additional condition is violated, for example at sufficiently small L , spatial-dispersion and intermode-interference effects may again become important and modify the line shape, even though strong damping is retained.

First, when $\Gamma \neq 0$, the transformation of the spectra of normal waves involves the transfer of energy through the crystal boundary into surface-radiative modes (including inhomogeneous ones). This determines the direct contribution of such modes to the total emission intensity at frequencies $\omega \leq \omega_L$.

Second, owing to the presence of spatial dispersion, interference interaction between mixed modes arises, which manifests itself in the formation of an additional interference energy flux at the crystal boundary.

The interference contribution to the luminescence intensity may become comparable, in absolute magnitude, with the individual contributions of the separate modes if the value of Γ and the emission angle θ of the radiation leaving the crystal satisfy the roots of the dispersion equation for radiative mixed modes. Third, at large values of Γ , when dissipative broadening becomes dominant and the additional condition for the quasiclassical regime is satisfied, the exciton luminescence spectrum of mixed modes approaches a Lorentzian form with a radiative-band half-width equal to Γ . In this case, the principal contribution to the total radiation from the two possible mixed modes is determined mainly by the exciton-like mixed mode for which the modulus of the wave vector (refractive index) has the minimum value.

The mechanism of formation of the considered MEPL spectra includes the elastic scattering of polaritons, initially in quantum states with sufficiently well-defined wave vectors, into the radiative states of mixed modes from relatively large $|\mathbf{k}|$ values. The distribution function of the scattered polaritons is characterized by an exponentially decaying spatial distribution described by the effective depth L . The value of L is determined unambiguously from the dependence of the position of the maximum luminescence spectral intensity on the emission angle θ . Here, L is in practice the only parameter of the theory that varies appreciably, since the values of all other parameters are determined from independent experimental data.

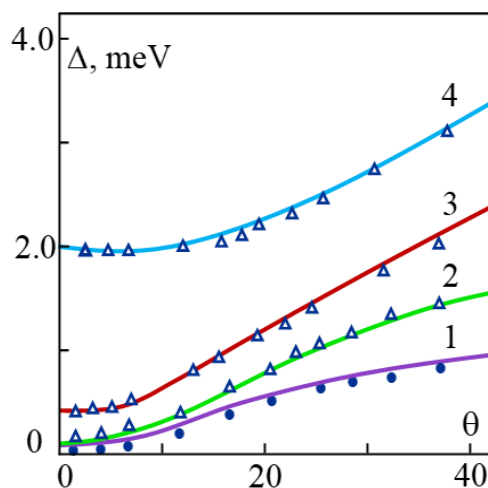


Figure 3. Dependence of the half-width Δ of the emission line of mixed modes in CdS crystals on the emission angle. The results are shown for temperatures $T = 4.5$ (1), 15 (2), 44 (3), and 77 (4) K. The points represent the experimental data, while the solid curves correspond to the theoretical calculations ($L = 1.5$ (1), 1.7 (2), 1.6 (3), 0.85 (4) μm ; $\hbar\Gamma = 0.1$ (1), 0.2 (2), 0.5 (3), 2.0 (4) meV).

CONCLUSIONS

In conclusion, the present work provides a comprehensive theoretical and experimental analysis of the formation mechanism of mixed exciton-polariton luminescence in CdS crystals under conditions of strong dissipative exciton damping. The obtained results make it possible to describe the dynamic behavior of excitons near the crystal surface, while fully accounting for the principal physical factors governing the radiation of mixed modes. The boundary conditions of the “crystal-external medium” interface employed in the theoretical model allow the emission process from the crystal surface to be explained at the microscopic level and are in good agreement with the available experimental data on specular and diffuse reflection of light for the CdS crystals under investigation [15-17].

The theoretical calculations made it possible to identify the principal features of mixed exciton-polariton luminescence spectra observed in the exciton-resonance region and to demonstrate their high degree of agreement with the experimental spectra. This

approach enables one to determine a physically well-grounded set of exciton resonance parameters and also makes it possible to reproduce with high accuracy the experimental MEPL spectra observed in the $E \perp c$ and $k \perp c$ configurations. Here, ccc denotes the direction of the sixfold principal optical axis of the crystal.

The results of this study show that, under conditions of strong exciton damping, the spectral contour of mixed-mode luminescence approaches a quasiclassical Lorentzian profile. However, in anisotropic crystals, spatial dispersion and intermode interference effects continue to play an important role in spectral formation. In particular, it has been established that subtle spectral features may arise due to the mutual superposition of two mixed modes and the contribution of a single pure longitudinal mode.

Thus, the obtained results contribute to a deeper understanding of the physical nature of mixed exciton-polariton luminescence in anisotropic semiconductor crystals of the CdS type and provide an important theoretical basis for describing radiative processes in strongly dissipative excitonic systems. This approach can be used as an effective tool for determining such physical quantities as exciton damping parameters, diffusion depth, and the half-width of the emission line.

ORCID

- © **Bozorboy J. Akhmadaliev**, <https://orcid.org/0000-0003-1930-8649>;
- © **Mekhriddin F. Akhmadjonov**, <https://orcid.org/0000-0002-1623-0404>;
- © **Tokhirbek I. Rakhmonov**, <https://orcid.org/0000-0002-6080-6159>;
- © **Paxlovon I. Movlonov**, <https://orcid.org/0009-0003-1380-9538>;
- © **Sherzod Sh. Abdullaev**, <https://orcid.org/0009-0007-9768-5008>;
- © **Iftikhorjon I. Yulchiev**, <https://orcid.org/0000-0001-9346-0441>

REFERENCES

- [1] S. Schumacher, G. Czycholl, and F. Jahnke, "Coherent propagation of polaritons in the nonlinear optical regime," *Physical Review B – Condensed Matter and Materials Physics*, **73**(3), 035318 (2006). <https://doi.org/10.1103/PhysRevB.73.035318>
- [2] J.J. Hopfield, and D.G. Thomas, "Polariton absorption lines," *Physical Review Letters*, **15**(1), 22-25 (1965). <https://doi.org/10.1103/PhysRevLett.15.22>
- [3] I. Carusotto, and C. Ciuti, "Quantum fluids of light," *Reviews of Modern Physics*, **85**(1), 299-366 (2013). <https://doi.org/10.1103/RevModPhys.85.299>
- [4] J. Voigt, "Influence of spatial dispersion on the transmission spectra of CdS single crystals," *Physica Status Solidi (b)*, **64**(2), 549-556 (1974). <https://doi.org/10.1002/pssb.2220640216>
- [5] Y. Tian, S. Yao, Z. Zhou, H. Peng, B. Ke, W. Zhou, *et al.*, "Super-Broad-Wavelength-Range Polarization-Selective Exciton-Polariton in Sn-Doped CdS Nanowires," *ACS Applied Optical Materials*, **1**(1), 298-305 (2023). <https://doi.org/10.1021/acsaom.2c00056>
- [6] V.V. Yatsyshen, and I.I. Borodina, "Reflection of circularly polarized light from a CdS semiconductor crystal near the exciton resonance taking into account spatial dispersion," *Physics of Wave Processes and Radio Systems*, **27**(4), 40-49 (2024). <https://doi.org/10.18469/1810-3189.2024.27.4.40-49>
- [7] D. Sanvitto, and S. Kéna-Cohen, "The road towards polaritonic devices," *Nature materials*, **15**(10), 1061-1073 (2016). <https://doi.org/10.1038/nmat4668>
- [8] M. Dagenais, and W.F. Sharfin, "Measurement of the damping dispersion of exciton polaritons in CdS," *Physical Review Letters*, **58**(17), 1776-1779 (1987). <https://doi.org/10.1103/PhysRevLett.58.1776>
- [9] F. Dirnberger, J. Quan, R. Bushati, G.M. Diederich, M. Florian, J. Klein, "Magneto-optics in a van der Waals magnet tuned by self-hybridized polaritons," *Nature*, **620**(7974), 533-537 (2023). <https://doi.org/10.1038/s41586-023-06275-2>
- [10] K.-H. Pantke, and I. Broser, "Damping dispersion of excitonic polaritons in CdS," *Physical Review B*, **48**(16), 11752-11758 (1993). <https://doi.org/10.1103/PhysRevB.48.11752>
- [11] P. Ghosh, D. Kushavah, P.K. Mohapatra, P. Vasa, K.C. Rustagi, and B.P. Singh, "Investigations of temperature-dependent photoluminescence of uncoated and silver-coated CdS quantum dots," <https://doi.org/10.48550/arXiv.1606.06711>
- [12] B.Zh. Akhmadaliev, N.Kh. Yuldashev, and I.I. Yulchiev, "Surface-radiative modes and longitudinal excitons in the spectra of exciton-polariton luminescence," *Optics and Spectroscopy*, **125**, 343-352 (2018). <https://doi.org/10.1134/S0030400X18090023>
- [13] B.Z. Akhmadaliev, and N.K. Yuldashev, "Strong Interference Luminescence of Mixed Modes in the Neighborhood of the Critical Value of Exciton Decay," *Optics and Spectroscopy*, **129**(11), 1187-1192 (2021). <https://doi.org/10.1134/S0030400X21090022>
- [14] N.N. Akhmediev, "Role of spatial dispersion in light absorption by excitons," *Soviet Journal of Experimental and Theoretical Physics*, **52**, 773 (1980). https://jetp.ras.ru/cgi-bin/dn/e_052_04_0773.pdf
- [15] A.B. Pevtsov, and A.V. Selkin, "Diffuse reflection of light in the region of exciton resonance in a CdS crystal," *Fizika Tverdogo Tela*, **26**(9), 2875-2877 (1984). <https://journals.ioffe.ru/articles/viewPDF/19256> (in Russian)
- [16] R.D. Delgado, V.A. Kosobukin, and A.V. Selkin, "Correlation effects of a rough crystal surface in exciton spectra of diffuse reflection," *Optics and Spectroscopy*, **63**(1), 6-8 (1987). <https://link.springer.com/article/10.1007/BF00654344>
- [17] N.R. Grigorieva, and A.V. Sel'kin, "Emission of Light from Compositionally Graded CdSe/CdS Heterostructure with Smooth Near-surface Excitonic Potential," *Semiconductors*, **53**(16), 2052-2054 (2019). <https://doi.org/10.1134/S1063782619120108>

ТЕОРЕТИЧНИЙ ТА ЕКСПЕРИМЕНТАЛЬНИЙ АНАЛІЗ ЛЮМІНЕСЦЕНЦІЇ ЗМІШАНИХ ЕКСИТОН-ПОЛЯРИТОНІВ У КРИСТАЛАХ CdS В УМОВАХ СИЛЬНОГО ЗАТУХАННЯ ЕКСИТОНІВ

Базарбой Дж. Ахмадалієв, Мехріддін Ф. Ахмаджонов, Тохірбек І. Рахмонов, Пахловон І. Мовлонов, Шерзод Ш. Абдуллаєв, Іфтїхорджон І. Юльчєв

Ферганський державний технічний університет, Фергана, Узбекистан

У даній роботі представлено комбіноване теоретичне та експериментальне дослідження люмінесценції змішаних екситон-поляритонів в анізотропних кристалах CdS у режимі сильного затухання екситонів поблизу резонансу А-екситона. Просторово-дисперсійна модель радіаційних змішаних мод використовується для аналізу трансформації спектрального контуру, положення максимуму, часткових мовових внесків та кутової залежності ширини лінії. Розраховані спектри для

кутів випромінювання від 10.4° до 85° порівнюються з вимірюваннями фотолюмінесценції, і отримано хорошу відповідність при температурі $T \approx 77$ К для $\hbar\Gamma = 2.0$ меВ та $L = 0.85$ мкм. На відміну від традиційних підходів, які пов'язують перехід до лоренцівського профілю випромінювання лише з умовою $\Gamma \gg \Gamma_c$, показано, що цей режим додатково вимагає виконання умови, пов'язаної з транспортом екситонів, а саме $2k_0L \cdot \text{Im}(n_{Mz}) \ll 1$. За виконання цих умов контур випромінювання змішаних мод наближається до квазікласичного лоренцівського профілю з напівшириною, близькою до $\hbar\Gamma$. Водночас у анізотропних кристалах *CdS* ефекти просторової дисперсії та міжмодової інтерференції не повністю пригнічуються і стають більш вираженими при більших кутах випромінювання або менших ефективних дифузійних довжинах. Отримані результати пропонують уточнений критерій ідентифікації квазікласичного режиму випромінювання та практичну основу для визначення параметра затухання екситонів і ефективної глибини дифузії з експериментальних спектрів.

Ключові слова: люмінесценція змішаних екситон-поляритонів; кристал *CdS*; сильне затухання екситонів; просторова дисперсія; анізотропний напівпровідник; змішані моди; резонанс *A*-екситона